Track-to-Track Association with Augmented State

RICHARD W. OSBORNE, III
YAAKOV BAR-SHALOM
PETER WILLETT

Association of tracks formed at different sensors is an ongoing area of interest in the field of information fusion and target tracking. In order to leverage additional information about a current target of interest that has been tracked at (an) additional sensor(s), track-to-track association (T2TA) must be performed. In addition to accurately identifying tracks with common origin, a desirable T2TA scheme will associate the tracks quickly, i.e., after only a few samples. A T2TA scheme is developed here that will take advantage of traditional kinematic state information as well as additional state information in the form of state augmentation. The main contribution is the use of two nonlinearly related state augmentations at the two sensors and accounting for their uncertainties. The results of T2TA are compared when using only kinematic state information, only state augmentation information, and the full augmented state. The full augmented state is shown to provide the most desirable association results, both in terms of accuracy and the number of samples needed to provide that accuracy.

Manuscript received May 13, 2011; revised September 7, 2011; released for publication October 19, 2011.

Refereeing of this contribution was handled by Stefano Coraluppi.

Authors' address: R. Osborne, III, Y. Bar-Shalom, and P. Willett, Department of Electrical and Computer Engineering, University of Connecticut, U-2157 Storrs, CT.

1557-6418/12/$17.00

1. INTRODUCTION

Proper application of data association is a key step in multitarget-multisensor tracking. For targets that travel over large distances, a single sensor can rarely survey the entire trajectory. For those sensors that are tracking targets which have previously been tracked (or are still being tracked) at other sensors, the prior information available from the previous tracks can prove valuable. In order to utilize any of the available information from previously formed tracks, accurate track-to-track association (T2TA) must be performed.

Previous literature [4] has developed T2TA using the kinematic states of each track to form the likelihood that two tracks share a common origin. Additionally, [8] provides a general framework for performing T2TA by combining any additional information about the target that may be available.

Since the kinematic information of each track can be formed into a likelihood function, additional information about each track can also be incorporated into the association by forming another likelihood function from the additional information. We will call this extra information the "state augmentation," and, when combined with the kinematic state of the track, the full state will be known as the "augmented state."

This work will examine a method of forming a likelihood ratio based cost for T2TA using the augmented state and an evaluation of the accuracy of the resulting T2TA. The state augmentation available at each sensor need not be identical in nature, but there must be a probabilistic relationship between them, so that the likelihood of tracks sharing a common origin can be formed. The case of two sensors' state augmentations which are nonlinearly related will be the focus of this work, along with a method to account for their uncertainties. This work will also show that the full augmented state T2TA provides significantly better association (more accurate and earlier association) than the kinematic information can provide alone.

Section 2 will formulate the problem and define some notation. Sections 3.1 and 3.2 will review the likelihood ratio based cost for association with kinematic information, as well as develop the likelihood ratio based cost for the state augmentation information. Section 3.3 will further develop the state augmentation association cost by taking into account the uncertain estimates of the state augmentation. Section 3.4 will present the full augmented state association cost. Section 4 presents the target motion model and earth model used to estimate and predict the kinematic states of the targets. Section 5 describes the sensor measurement noise assumptions and necessary measurement conversions. Section 6 will present the simulation scenarios and result, and Section 7 will present the conclusions.

2. PROBLEM FORMULATION

A total of M sensors are assumed to track N targets, with trajectories which pass into and out of the

surveillance regions of each sensor. Each sensor will individually form kinematic tracks on each target and provide additional information which will augment the kinematic state. Each target and sensor is assumed to follow a motion and measurement model of the form

$$x(k+1) = f(x(k)) + v(k) \tag{1}$$

$$z(k) = h(x(k)) + w(k) \tag{2}$$

where $x(k)$ is the kinematic state at time k, $z(k)$ is the measurement at time k, $v(k)$ is the process noise, and $w(k)$ is the measurement noise.

The full augmented state estimate of target i available from sensor m is

$$\hat{\mathbf{x}}_m^i(k) = \begin{bmatrix} \hat{x}_m^i(k) \\ \hat{y}_m^i(k) \end{bmatrix} \tag{3}$$

where $\hat{x}_m^i(k)$ is the estimate of the kinematic state of target i from sensor m. The quantity $\hat{y}_m^i(k)$ is the corresponding estimated state augmentation vector

$$y_m^i(k) = [\zeta_m^{i,1}(k), \zeta_m^{i,2}(k), \ldots, \zeta_m^{i,n}(k)]' \tag{4}$$

available at sensor m, consisting of n elements. The number of elements n need not be the same between sensors and may also be measures of different quantities entirely. The necessary information is the probabilistic relationship between the state augmentation at each sensor. For the case of $M = 2$, the association will be carried out by taking advantage of the pdf (probability density function) of the state augmentation at the second sensor conditioned on the augmentation at the first sensor and the target's kinematic state under the "common origin" assumption, i.e.,

$$p[y_2 \mid y_1, x^i] \tag{5}$$

For the purposes of this work, the kinematic state will be defined as a target's position and velocity components (in Cartesian coordinates). The second sensor's state augmentation will be the target's reflectivity.

The state augmentation likelihood ratio cost will be developed in Section 3.2 assuming $\hat{y}_m^i(k)$ is a known quantity, while Section 3.3 will present the case where $\hat{y}_m^i(k)$ is a vector of random variables.

In order to form the cost of associating two tracks from different sensors, the likelihood function of the tracks having common origin is needed. The likelihood function [3] of a parameter θ is defined as $p(z \mid \theta)$, where z denotes the observations. The maximum likelihood estimate of θ is then

$$\hat{\theta}^{ML}(z) = \arg\max_{\theta} p(z \mid \theta) \tag{6}$$

In the case of measurement-to-track association (M2TA) the observation will be the measurement [1], while for T2TA, the observation will be the kinematic state [2] and/or the state augmentation.

The cost of association requires a likelihood ratio in order to differentiate between common and disparate origin. Furthermore, in order to be a valid cost function, the cost of association should be the negative of the likelihood ratio. For these reasons, the cost will be given by the negative log-likelihood ratio (NLLR)

$$\text{NLLR} = -\ln\left\{\frac{p(z \mid \text{“common origin”})}{p(z \mid \text{“different origin”})}\right\} \triangleq \mathcal{L} \tag{7}$$

Minimizing the sum of the NLLRs for all the associations will provide the overall T2TA.

3. AUGMENTED STATE T2TA

The sequel will assume that T2TA takes place between two sensors ($M = 2$) to simplify the explanation of the costs, but the generalization to more than two sensors is straightforward. Each sensor will provide a list of tracks which are to be associated, and there exist a number of good methods to perform the assignment once the costs are obtained [6], [7], [12], [13]. For the two sensor case, a 2-D assignment algorithm such as the auction algorithm works quite well.

To perform the overall track association, the joint likelihood of two tracks having common origin is required. The joint likelihood of track j at the second sensor having originated from the same target as track i at the first sensor—assuming that the kinematic and state augmentation information are independent—is simply

$$\Lambda^{ij}(k) = \Lambda_x^{ij}(k)\Lambda_y^{ij}(k) \tag{8}$$

where $\Lambda_x^{ij}(k)$ is the kinematic likelihood and $\Lambda_y^{ij}(k)$ is the state augmentation likelihood.

3.1. Kinematic State T2TA

The kinematic likelihood of two tracks sharing a common origin has been derived previously [4], but will be briefly reviewed here. In order to determine if two tracks pertain to the same target using their kinematic information, the states can be directly compared. In some cases, the estimated state from one sensor may no longer be available (e.g., the target may be outside the first sensor's surveillance region). In that case, the predicted state may be used instead.

For two tracks which originated from the same target, the true states are equal, i.e.,

$$\Delta^{ij}(k) = x^i(k) - x^j(k) = 0 \tag{9}$$

The error of the state estimate difference is

$$\tilde{\Delta}^{ij}(k) = \tilde{x}^i(k) - \tilde{x}^j(k) \tag{10}$$

where $\tilde{x}^i(k)$ and $\tilde{x}^j(k)$ are the errors in the estimated states of track i and j, respectively. Assuming $\tilde{x}^i(k)$ and $\tilde{x}^j(k)$ are zero-mean, $\tilde{\Delta}^{ij}$ will also be zero-mean. The covariance of $\tilde{\Delta}^{ij}(k)$ is

$$T^{ij}(k) = E\{[\tilde{x}^i(k) - \tilde{x}^j(k)][\tilde{x}^i(k) - \tilde{x}^j(k)]'\} \tag{11}$$

$$= P^i(k) + P^j(k) - P^{ij}(k) - P^{ji}(k) \tag{12}$$

where P^i is the covariance of track i (at sensor 1), P^j is the covariance of track j (at sensor 2), and $P^{ij} = (P^{ji})'$ is the crosscovariance of tracks i and j [4]. Assuming the state estimation errors are Gaussian, the kinematic

state likelihood function will be [2]

$$\Lambda_x^{ij}(k) = \frac{1}{|2\pi T^{ij}(k)|^{1/2}} \cdot \exp\left[-\frac{1}{2}(\hat{x}^i(k) - \hat{x}^j(k))'[T^{ij}(k)]^{-1}(\hat{x}^i(k) - \hat{x}^j(k))\right] \tag{13}$$

As stated previously, the cost used for the association is provided by a (dimensionless) likelihood ratio (specifically, the NLLR). This allows for the complete assignment of all the tracks from lists of different lengths, by allowing assignment of tracks to so called "dummy" tracks. The kinematic state likelihood function for assignment of a track to a nonexistent dummy track is

$$\Lambda_x^{0j}(k) = \lambda_{\text{ex}} \tag{14}$$

where the dummy track is indexed by $i = 0$ and λ_{ex} is the spatial density of extraneous tracks seen by the second sensor (i.e., false or new tracks) [2].

The NLLR resulting from (13) and (14) is

$$\begin{aligned}\mathcal{L}_x^{ij}(k) &\triangleq -\ln\frac{\Lambda_x^{ij}(k)}{\Lambda_x^{0j}(k)} \\ &= \frac{1}{2}(\hat{x}^i(k) - \hat{x}^j(k))'[T^{ij}(k)]^{-1}(\hat{x}^i(k) - \hat{x}^j(k)) \\ &\quad + \ln(\lambda_{\text{ex}}|2\pi T^{ij}(k)|^{1/2})\end{aligned} \tag{15}$$

The overall cost of association using kinematic state information will explicitly handle the cases where dummy tracks are necessary, and is defined as

$$C_x^{ij}(k) = \begin{cases} \mathcal{L}_x^{ij}(k) & \text{if} \quad i,j \neq 0 \\ -\ln(1 - P_{D_1}) & \text{if} \quad i = 0, \quad j \neq 0 \\ -\ln(1 - P_{D_2}) & \text{if} \quad i \neq 0, \quad j = 0 \end{cases} \tag{16}$$

where P_{D_m} is the track detection probability of the mth sensor.

3.2. State Augmentation T2TA

The likelihood of two tracks sharing a common origin using state augmentation information will now be derived. To illustrate the derivation, a specific example where the state augmentation $y_2^j(k)$ at the second sensor follows a Swerling 1 distribution will be used. In this case, the pdf of $y_2^j(k)$ is

$$p(y_2^j(k) \mid y_1^i) = \frac{1}{\bar{y}_2(g[y_1^i, \hat{x}^j(k)])} \exp\left\{-\frac{y_2^j(k)}{\bar{y}_2(g[y_1^i, \hat{x}^j(k)])}\right\} \tag{17}$$

where the (possibly nonlinear) function $\bar{y}_2(\cdot)$ is the predicted value of $y_2^j(k)$ and $g(\cdot)$ is a (possibly nonlinear) function of the first sensor's state augmentation.

The likelihood function of tracks i and j having common origin, using data over a window of length L_w, assuming $y_2^j(k)$ is independent across samples (due to the Swerling 1 assumption), is

$$\begin{aligned}\Lambda_y^{ij}(k) &= \prod_{l=k-L_w+1}^{k} \frac{1}{\bar{y}_2(g[y_1^i, \hat{x}^j(l)])} \cdot \exp\left\{-\frac{y_2^j(l)}{\bar{y}_2(g[y_1^i, \hat{x}^j(l)])}\right\} \\ &= \frac{1}{\prod_{l=k-L_w+1}^{k} \bar{y}_2(g[y_1^i, \hat{x}^j(l)])} \cdot \exp\left\{-\sum_{l=k-L_w+1}^{k} \frac{y_2^j(l)}{\bar{y}_2(g[y_1^i, \hat{x}^j(l)])}\right\}\end{aligned} \tag{18}$$

The likelihood function of (18) will provide the numerator of the likelihood ratio, and the likelihood of an assignment of a track at the second sensor to a dummy track will be the denominator. Such a likelihood will be given by

$$\begin{aligned}\Lambda_y^{0j}(k) &= \prod_{l=k-L_w+1}^{k} \frac{1}{\bar{y}_0^j(k)} \exp\left\{-\frac{y_2^j(l)}{\bar{y}_0^j(k)}\right\} \\ &= \frac{1}{(\bar{y}_0^j(k))^{L_w}} \exp\left\{-\sum_{l=k-L_w+1}^{k} \frac{y_2^j(l)}{\bar{y}_0^j(k)}\right\}\end{aligned} \tag{19}$$

where $\bar{y}_0^j(k)$ is the average of the observed y_2^j within a window of length L_w ending at k (i.e., the average of an "extraneous origin" [1] signal)

$$\bar{y}_0^j(k) = \frac{1}{L_w} \sum_{l=k-L_w+1}^{k} y_2^j(l) \tag{20}$$

The NLLR resulting from (18) and (19) is

$$\begin{aligned}\mathcal{L}_y^{ij}(k) &\triangleq -\ln\frac{\Lambda_y^{ij}(k)}{\Lambda_y^{0j}(k)} \\ &= -L_w \ln(\bar{y}_0^j(k)) - \sum_{l=k-L_w+1}^{k} \frac{y_2^j(l)}{\bar{y}_0^j(k)} \\ &\quad - \frac{y_2^j(l)}{\bar{y}_2(g[y_1^i, \hat{x}^j(l)])} - \ln[\bar{y}_2(g[y_1^i, \hat{x}^j(l)])]\end{aligned} \tag{21}$$

The overall cost of association using state augmentation information will, once again, explicitly handle the cases where dummy tracks are necessary, and is defined as

$$C_y^{ij}(k) = \begin{cases} \mathcal{L}_y^{ij}(k) & \text{if} \quad i,j \neq 0 \\ -\ln(1 - P_{D_1}) & \text{if} \quad i = 0, \quad j \neq 0 \\ -\ln(1 - P_{D_2}) & \text{if} \quad i \neq 0, \quad j = 0 \end{cases} \tag{22}$$

where P_{D_m} is the track detection probability of the mth sensor.

3.3 Modified Cost Function for Uncertainty in the Estimated State Augmentation

The previous section derived the cost of association based on state augmentation information by implicitly assuming that the first sensor's state augmentation was a known quantity. In reality, the first sensor will only be able to estimate the state augmentation, and the overall association can be improved by accounting for this uncertainty. To account for the uncertainty, the expected value of (17) will be used in the calculation of the state augmentation cost. In general, the function $g(\cdot)$—which determines the expected value of the second sensor's state augmentation and is itself a function of the first sensor's *estimated* state augmentation $\hat{y}_1^i$—is nonlinear. The expectation of (17) over y_1^i will, therefore, be handled by an unscented transform [9] and is

$$\begin{aligned} E_{y_1^i}[p(y_2^j(k) \mid y_1^i)] &= \int p(y_2^j(k) \mid y_1^i) p(y_1^i) dy_1^i \\ &= \int p(y_2^j(k) \mid g(\hat{y}_1^i, \hat{x}^j(k))) p(y_1^i) dy_1^i \end{aligned} \tag{23}$$

where $g(\hat{y}_1^i, \hat{x}^j(k))$ is the mapping of the state augmentation from sensor 1 to the state augmentation of sensor 2 (i.e., the sufficient statistic for the predicted state augmentation at sensor 2, which is the target reflectivity) at the position component of $\hat{x}^j(k)$.

This is approximated by using a probability mass function

$$E_{y_1^i}[p(y_2^j(k) \mid y_1^i)] \approx \sum_{m=-n}^{n} p(y_2^j(k) \mid g(y_{1m}^i, \hat{x}^j(k))) \mu(y_{1m}^i) \tag{24}$$

where n is the dimension of y_1^i and $\mu(y_{1m}^i)$ are the weights (point masses) of the $2n + 1$ points used in the unscented transform [9].

In the case of $n = 5$, the points and weights will be

$$\begin{aligned} y_{1m}^i &= \hat{y}_1^i + \text{sgn}(m)\sqrt{7}\sigma_m \\ \mu(y_{1m}^i) &= \begin{cases} 1/14 & \text{if} \quad m \neq 0 \\ 2/7 & \text{if} \quad m = 0 \end{cases} \end{aligned} \tag{25}$$

where $\hat{y}_1^i$ is the state augmentation handed over from the first sensor, and σ_m is the standard deviation for the mth element of $\hat{y}_1^i$.

The weights for each point of the unscented transform according to [9] should be

$$\mu_m = \begin{cases} \kappa/(n+\kappa) & \text{if} \quad m = 0 \\ 1/2(n+\kappa) & \text{if} \quad m \neq 0 \end{cases} \tag{26}$$

where κ is an extra degree of freedom for "fine tuning" the approximation. In this case, $\kappa = 2$ was chosen, since, for a one dimensional Gaussian distribution, that particular choice of κ will provide an approximation which coincides to matching the second and fourth moments of the Gaussian distribution.[1]

[1]The authors of [9] suggest using $n + \kappa = 3$ for a Gaussian distribution, but this would give rise, for $n = 5$, to a nonsensical negative weight for the center point of the approximation.

Utilizing the unscented transform, the state augmentation cost function will be calculated as in Section 3.2, replacing (17) with (24).

3.4. Full Augmented State T2TA

In light of the previous derivations, the cost of the association using the full augmented state can now be fully specified. Assuming the kinematic and state augmentation information is independent, the full augmented state cost is [4]

$$C^{ij}(k) = \begin{cases} \mathcal{L}_x^{ij}(k) + \mathcal{L}_y^{ij}(k) & \text{if } i, j \neq 0 \\ -\ln(1 - P_{D_1}) & \text{if } i = 0, \quad j \neq 0 \\ -\ln(1 - P_{D_2}) & \text{if } i \neq 0, \quad j = 0 \end{cases} \tag{27}$$

Note that the costs in lines 2 and 3 of (27) are not the sums of the corresponding lines of (16) and (22), since, if a detection is missing, both point kinematic and state augmentation are missing.

With the NLLR costs fully specified, the two dimensional assignment of tracks from the first sensor to tracks at the second sensor—each list with a dummy track added—can now be carried out using the auction algorithm (for a review of the auction algorithm see [12]).

4. TARGET MOTION MODEL

In order to estimate and predict the target state for use in the kinematic cost function, an appropriate target motion model is necessary. All tracking performed here is assumed to be done on targets which are under the influence of gravity alone. Since gravity is the only force acting on the targets, the gravitational pull of the earth must be accurately modeled.

An ellipsoidal earth model with a single zonal harmonic term will be used to model the acceleration of a target due to the earth's gravity [5], [10]. Additionally, the tracking is assumed to be done in the earth-centered-inertial (ECI) coordinate system, which avoids the need to calculate accelerations due to Coriolis and centrifugal forces caused by the earth's rotation if an earth-fixed coordinate system were used. The acceleration due to gravity using this ellipsoidal earth model is

$$\begin{aligned} \mathbf{a}(\mathbf{p}) &\triangleq \begin{bmatrix} \ddot{x} \\ \ddot{y} \\ \ddot{z} \end{bmatrix} \\ &= -\frac{\mu}{p^3} \begin{bmatrix} \left(1 + \frac{3J_2 r_e^2}{2p^2}\left(1 - 5\frac{z^2}{p^2}\right)\right) x \\ \left(1 + \frac{3J_2 r_e^2}{2p^2}\left(1 - 5\frac{z^2}{p^2}\right)\right) y \\ \left(1 + \frac{3J_2 r_e^2}{2p^2}\left(3 - 5\frac{z^2}{p^2}\right)\right) z \end{bmatrix} \end{aligned} \tag{28}$$

where $\mu = 398601.2\ \text{km}^3/\text{s}^2$ is earth's gravitation constant, $J_2 = 1.0826 \times 10^{-3}$ is the first zonal harmonic term, r_e is the equatorial radius of the earth (using the WGS84 earth model, $r_e = 6378.137$ km), and $p = \|\mathbf{p}\|$ where $\mathbf{p} = [x, y, z]'$.

The target motion model which will be assumed for estimation and prediction will be a discretized continuous white noise acceleration model (DCWNA), with the acceleration due to earth's gravity assumed piecewise constant and entering the motion model as a known input. The acceleration at each sampling time will be given by (28) evaluated at the current measurement of the target's position (if a current measurement is not available, the predicted state will instead be used). Given the state $\mathbf{x}(k)$ at time k, where $\mathbf{x}(k) \triangleq [x(k), y(k), z(k), \dot{x}(k), \dot{y}(k), \dot{z}(k)]'$ and is given in ECI coordinates, the state $\mathbf{x}(k+1)$ is

$$\mathbf{x}(k+1) = F\mathbf{x}(k) + G\mathbf{a}(\mathbf{p}(k)) + v(k) \tag{29}$$

where

$$F = \begin{bmatrix} I_3 & I_3 T \\ 0 & I_3 \end{bmatrix}, \qquad G = \begin{bmatrix} I_3 \dfrac{T^2}{2} \\ I_3 T \end{bmatrix} \tag{30}$$

I_3 is the 3×3 identity matrix, $\mathbf{p}(k)$ is the target position (given by measurement or predicted state) at time k and $v(k)$ is the process noise.

Since the targets are all assumed to be under the influence of gravity alone, a very small process noise should be sufficient. The covariance of the process noise $v(k)$ is given by

$$Q = \begin{bmatrix} I_3 \dfrac{T^3}{3} & I_3 \dfrac{T^2}{2} \\ I_3 \dfrac{T^2}{2} & I_3 T \end{bmatrix} q \tag{31}$$

The intensity (power spectral density) of the process noise q chosen for this motion model was $0.01\ \text{m}^2/\text{s}^3$.

The target tracking will be performed using a standard Kalman filter [3] with the above motion model. The prediction from the end of the first sensor's tracks to the time the second sensor begins tracking will be done using the same DCWNA model with the acceleration due to gravity given by (28).

5. SENSOR MEASUREMENT NOISE AND MEASUREMENT CONVERSION

While the target measurements used in the Kalman filter will be in ECI coordinates, the measurement noise will be added to the measurements in terms of range, azimuth and elevation. The measurement of the target is given by

$$r_m = r + w_r, \qquad a_m = a + w_a, \qquad \epsilon_m = \epsilon + w_\epsilon \tag{32}$$

where r, a and ϵ are the true range, azimuth and elevation angles, respectively, and w_r, w_a and w_ϵ are independent zero-mean Gaussian noise with standard deviations σ_r, σ_a and σ_ϵ, respectively.

TABLE I
Measurement Noise Standard Deviations for Both Sensors
(The Handover was from Sensor 1 to Sensor 2)

	Range σ_r (m)	Azimuth σ_α (mrad)	Elevation σ_ϵ (mrad)
Scenario 1	10	0.5	0.5
Scenario 2	20	1	1

TABLE II
State Augmentation Estimation Error Standard Deviations

	σ_{ζ_1}	σ_{ζ_2}	σ_{ζ_3}	σ_{ζ_4}	σ_{ζ_5}
Scenario A	17.5	17.5	17.5	0.087	17.5
Scenario B	52.5	52.5	52.5	0.087	52.5
Scenario C	52.5	52.5	52.5	0.140	52.5

These measurements must be converted to ECI coordinates in order to be used by the Kalman filter which uses the models outlined in Section 4. The measurements should first be converted to a Cartesian coordinate system aligned with the sensor face plane, and then rotated and translated to match the ECI coordinate system. Since the range from the sensor to the targets is very large, there is a possibly significant bias that can be introduced in the conversion from spherical coordinates to Cartesian. The unbiased conversion [11] will, therefore, be used.

The covariance matrix in ECI coordinates, R_e, will then be

$$R_e = T(k)' R_r T(k) \tag{33}$$

where $T(k)$ is the transformation matrix used to rotate from ECI coordinates to sensor face coordinates at time k and R_r is the covariance matrix of the unbiased converted measurements.

6. SIMULATION RESULTS

The scenarios considered consist of 6 targets under the influence of gravity alone. The two sensors are both assumed to measure reflectivity, but have different sampling intervals. The first sensor tracks the targets over approximately 520 samples (some of the targets have a few extra samples at the beginning or end of the track). The interval between the time the first sensor stops tracking and the second sensor begins tracking is approximately 1500 sampling intervals. The second sensor tracks the targets over approximately 1060 samples. The targets at all times are separated by more than $40\sigma_r$, i.e., they are resolved. The measurement noise standard deviations of the two sensors are given in Table I.

Additionally, the $n = 5$ elements of y_1^i estimated for each track at the first sensor are assumed to have zero-mean Gaussian errors with standard deviations given in Table II. The scenarios will be designated as 1A–1C and 2A–2C.

Each figure shows the average association accuracy (i.e., fraction of tracks correctly identified as having common origin), averaged over 200 runs. Three association accuracy plots are shown in each figure: the association accuracy using only the kinematic cost (16), the association accuracy using only the state augmentation cost (22), and the association accuracy using the full augmented state cost (27).

Figures 1–3 show the association accuracy for scenarios 1A–1C, respectively (with measurement noise standard deviations given by scenario 1 of Table I, and state augmentation error standard deviations given by scenarios A–C of Table II) with window length $L_w = 100$.

Figures 4–6 show the association accuracy for scenarios identical to figures 1–3, however, the unscented evaluation of the state augmentation costs have been used.

Figures 7–9 show the association accuracy for scenarios 1A–1C, respectively (with measurement noise standard deviations given by scenario 1 of Table I, and state augmentation error standard deviations given by scenarios A–C of Table II) with window length $L_w = 200$.

Figures 10–12 show the association accuracy for scenarios identical to figures 7–9, however, the unscented evaluation of the state augmentation costs have been used.

Figures 13–15 show the association accuracy for scenarios 2A–2C, respectively (with measurement noise standard deviations given by scenario 2 of Table I, and target state augmentation error standard deviations given by scenarios A–C of Table II) with window length $L_w = 100$.

Figures 16–18 show the association accuracy for scenarios identical to figures 13–15, however, the unscented evaluation of the state augmentation costs have been used.

Figures 19–21 show the association accuracy for scenarios 2A–2C, respectively (with measurement noise standard deviations given by scenario 2 of Table I, and target state augmentation error standard deviations given by scenarios A–C of Table II) with window length $L_w = 200$.

Figures 22–24 show the association accuracy for scenarios identical to figures 19–21, however, the unscented evaluation of the state augmentation costs have been used.

When the measurement noise is large, the accuracy of the kinematic tracking will suffer, and the kinematic-only association will remain accurate, but will take longer to achieve high accuracy. The accuracy of the state augmentation only association remains relatively unaffected by the highest measurement noise (scenario 2), but even higher noise could begin to affect the accuracy because of inaccurate target positions used in determining the aspect angles of the targets.

The higher levels of state augmentation estimation uncertainty can degrade the performance of the augmentation association enough to cause the combined association to perform worse than the association using kinematic information alone. The use of very inaccurate state augmentation variables clouds the picture by flattening the likelihoods, and deteriorates the association accuracy. A larger window size of $L_w = 200$ can improve the association somewhat and prevent some degradation of the combined accuracy for the higher levels of state augmentation estimation error, as seen in Figs. 7–12 and 19–24. Ultimately, the overall accuracy is very sensitive to the state augmentation estimation accuracy.

Figures 4–6, 10–12, 16–18, and 22–24, however, show that the unscented transform can improve the overall accuracy for the cases of higher state augmentation estimation errors by taking into account the uncertainty of the estimation.

The scenarios with higher measurement noisepresent some interesting results for the early portions of the second sensor's tracks. The association based on only kinematic information will completely fail to accurately associate any of the second sensor's targets for the early portion of the trajectories. The augmentation-only association will perform more accurately than kinematic-only association for those early portions, but will not perform as well as desired. Once the two costs, which work poorly alone, are combined, however, the association is extremely accurate. The reason for this is the kinematic information results in a cost function which favors assigning the second sensor's tracks to dummy tracks for the early portions of the trajectories. This results in the very poor association accuracy in the kinematic-only association. The augmentation-only association results in costs which favor the actual tracks over dummy tracks, but has difficulty correctly distinguishing among the true tracks. When the negative costs from the augmentation portion are added to the kinematic costs, however, the total costs no longer favor dummy tracks (due to the augmented state information) and are still distinguishable from early portions of the trajectories (due to the kinematic information).

Even when the measurement noise standard deviations are small (in which case the kinematic-only association performs very well), the addition of the state augmentation into the association improves the accuracy of the T2TA, resulting in a near perfect association very quickly after the targets are tracked at the second sensor. The use of the state augmentation cost also improves T2TA accuracy even though the augmentation-only association is less accurate than the kinematic-only association. When the measurement noise standard deviations are larger, the addition of the state augmentation cost helps to improve the overall T2TA, even during portions of the track when the kinematic-only association performs very poorly.

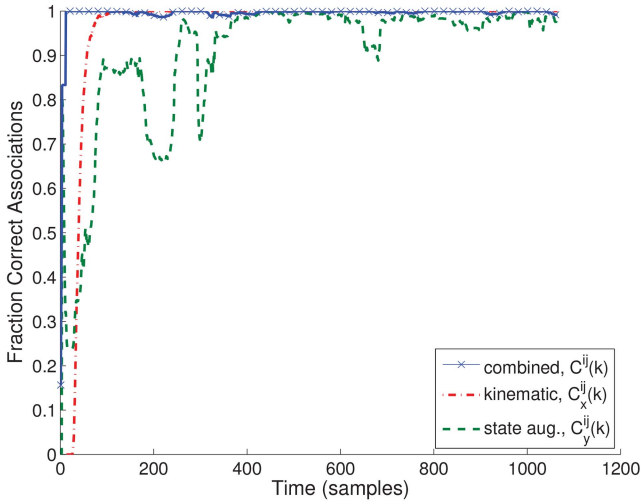

Fig. 1. Average association accuracy over 200 runs (scenario 1A), with window length L_w = 100.

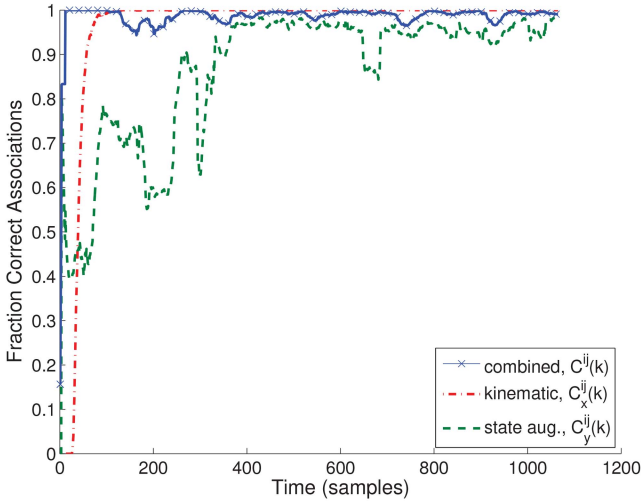

Fig. 2. Average association accuracy over 200 runs (scenario 1B), with window length L_w = 100.

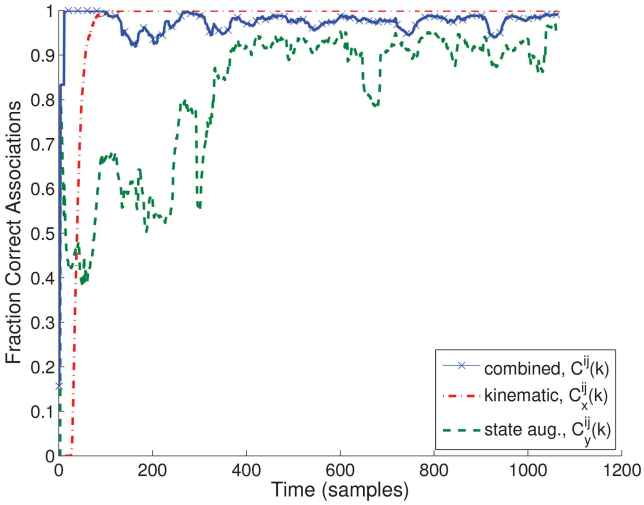

Fig. 3. Average association accuracy over 200 runs (scenario 1C), with window length L_w = 100.

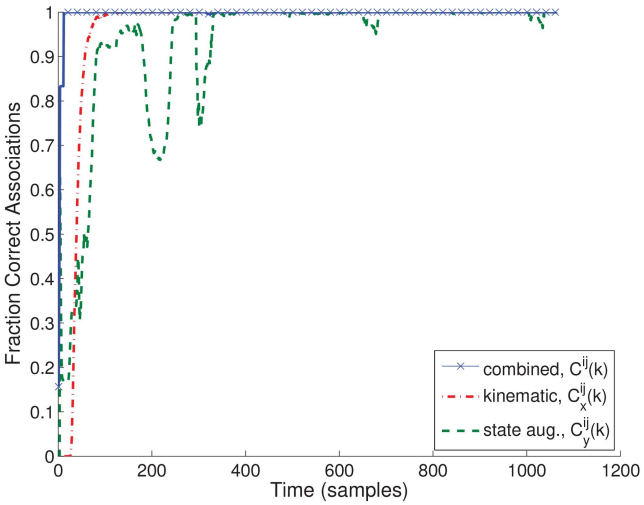

Fig. 4. Average association accuracy over 200 runs with unscented state augmentation costs (scenario 1A), window length L_w = 100.

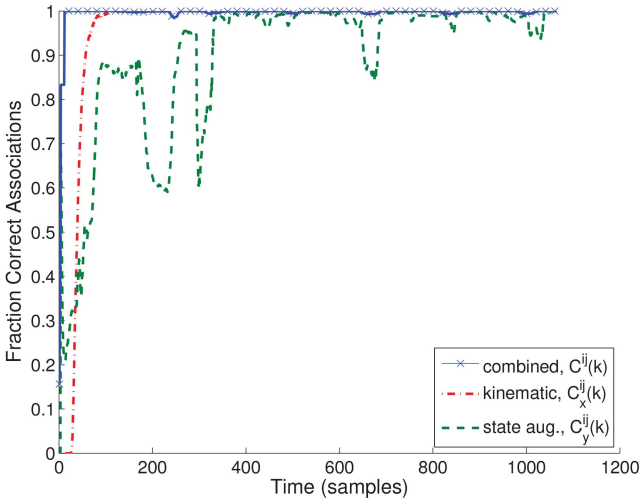

Fig. 5. Average association accuracy over 200 runs with unscented state augmentation costs (scenario 1B), window length L_w = 100.

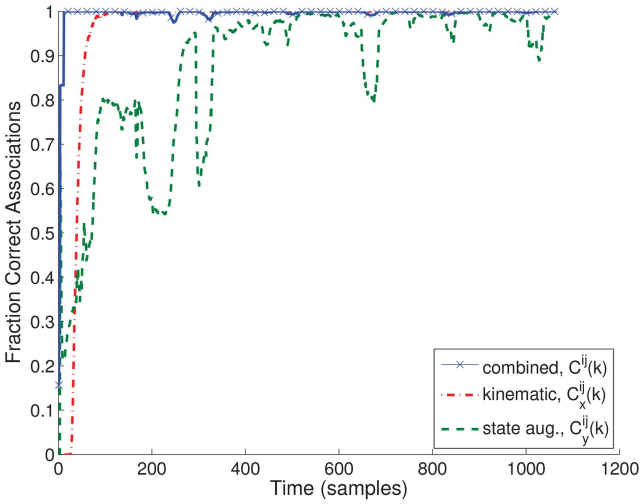

Fig. 6. Average association accuracy over 200 runs with unscented state augmentation costs (scenario 1C), window length L_w = 100.

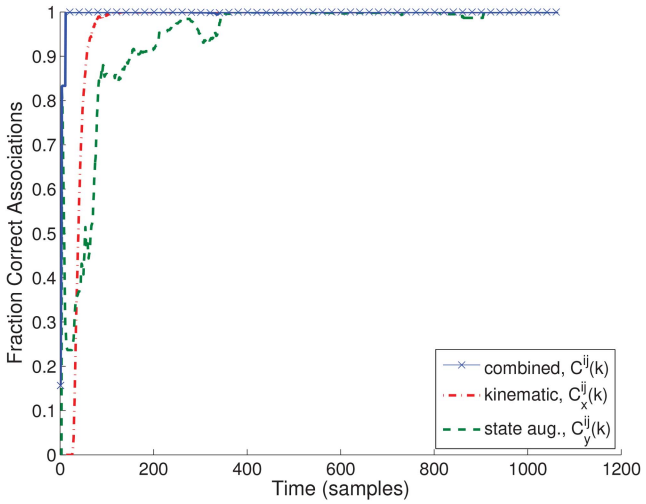

Fig. 7. Average association accuracy over 200 runs (scenario 1A), with window length $L_w = 200$.

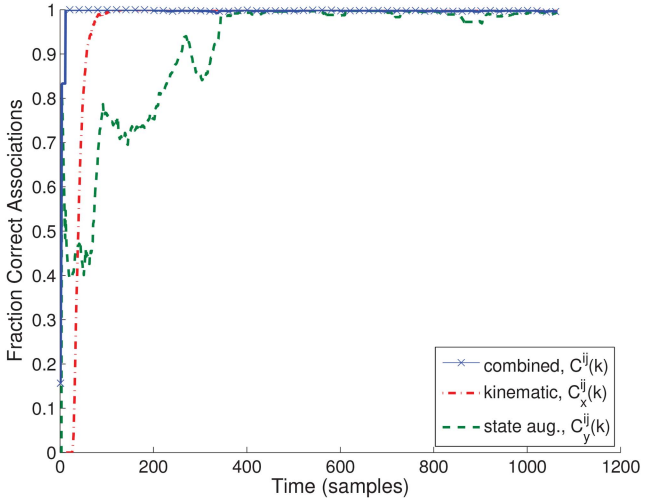

Fig. 8. Average association accuracy over 200 runs (scenario 1B), with window length $L_w = 200$.

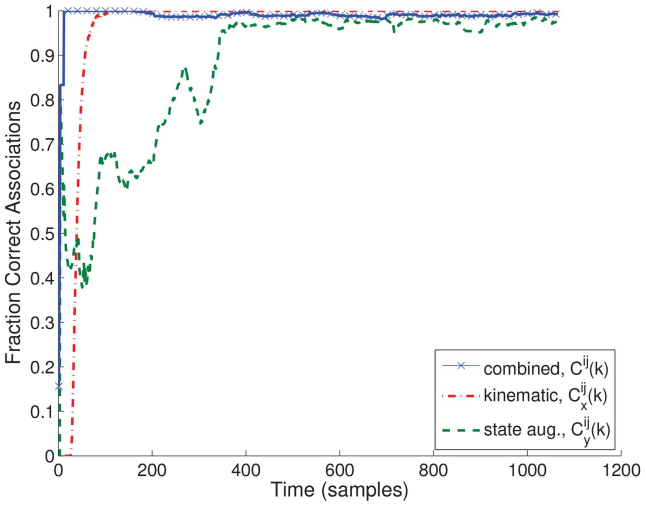

Fig. 9. Average association accuracy over 200 runs (scenario 1C), with window length $L_w = 200$.

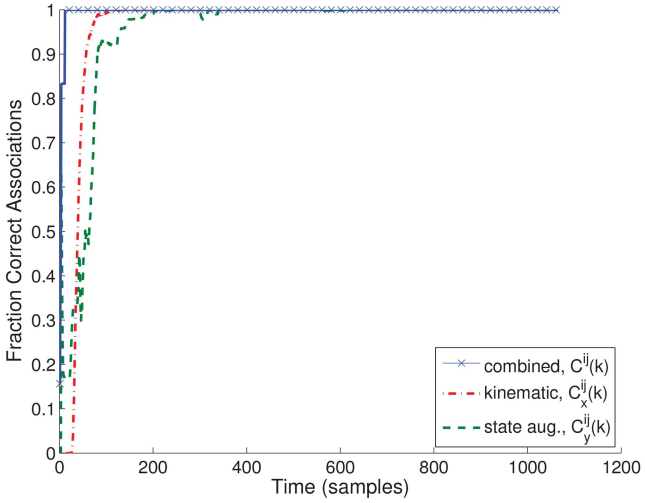

Fig. 10. Average association accuracy over 200 runs with unscented state augmentation costs (scenario 1A), window length $L_w = 200$.

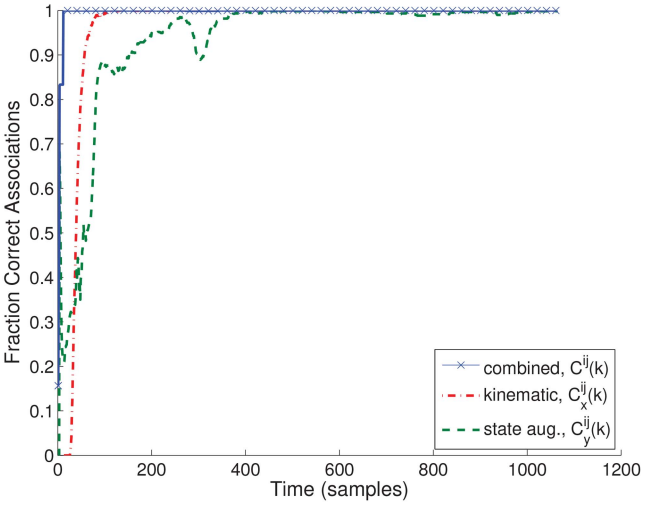

Fig. 11. Average association accuracy over 200 runs with unscented state augmentation costs (scenario 1B), window length $L_w = 200$.

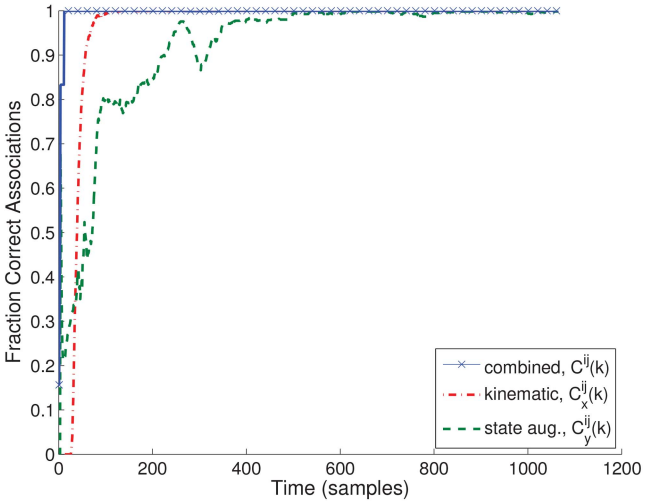

Fig. 12. Average association accuracy over 200 runs with unscented state augmentation costs (scenario 1C), window length $L_w = 200$.

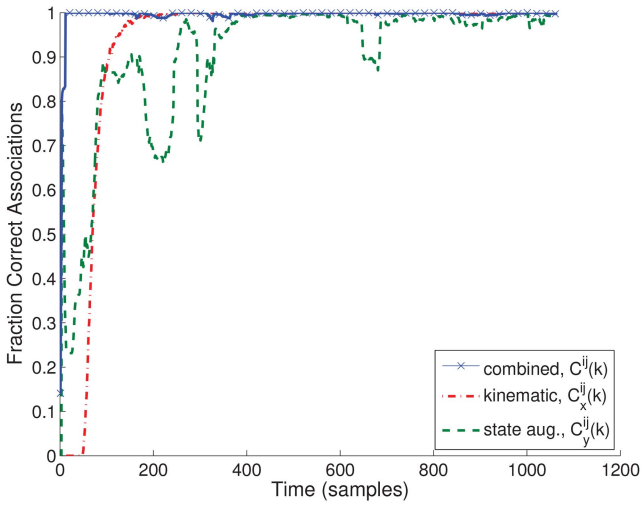

Fig. 13. Average association accuracy over 200 runs (scenario 2A), with window length $L_w = 100$.

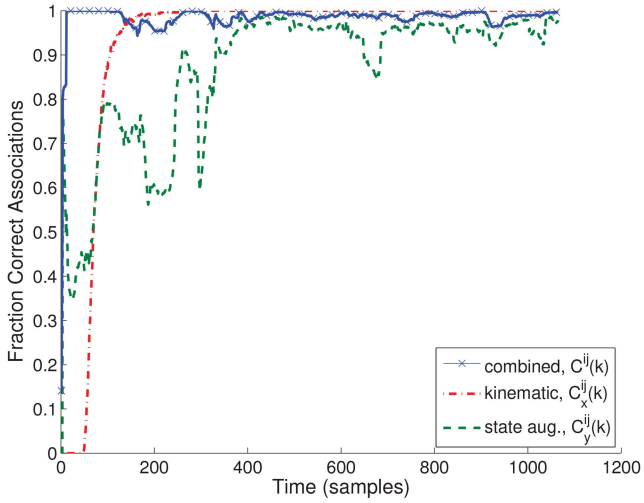

Fig. 14. Average association accuracy over 200 runs (scenario 2B), with window length $L_w = 100$.

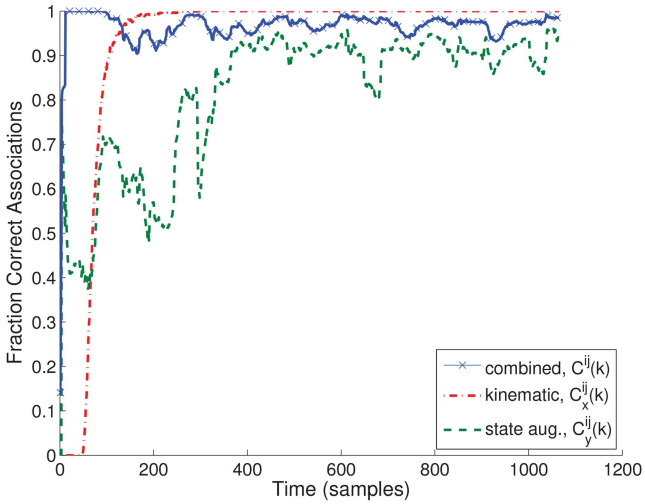

Fig. 15. Average association accuracy over 200 runs (scenario 2C), with window length $L_w = 100$.

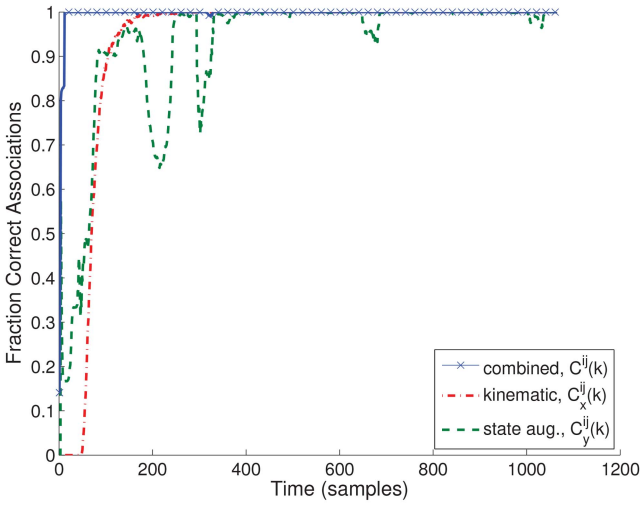

Fig. 16. Average association accuracy over 200 runs with unscented state augmentation costs (scenario 2A), window length $L_w = 100$.

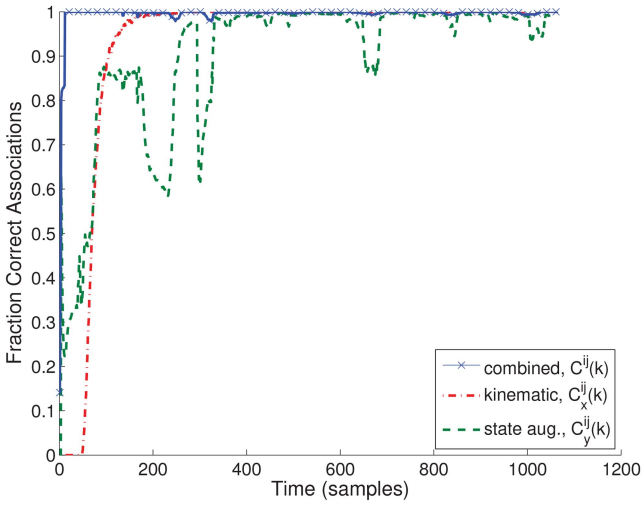

Fig. 17. Average association accuracy over 200 runs with unscented state augmentation costs (scenario 2B), window length $L_w = 100$.

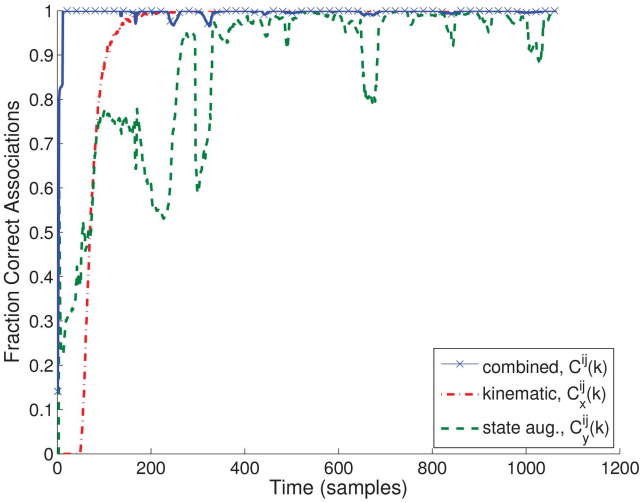

Fig. 18. Average association accuracy over 200 runs with unscented state augmentation costs (scenario 2C), window length $L_w = 100$.

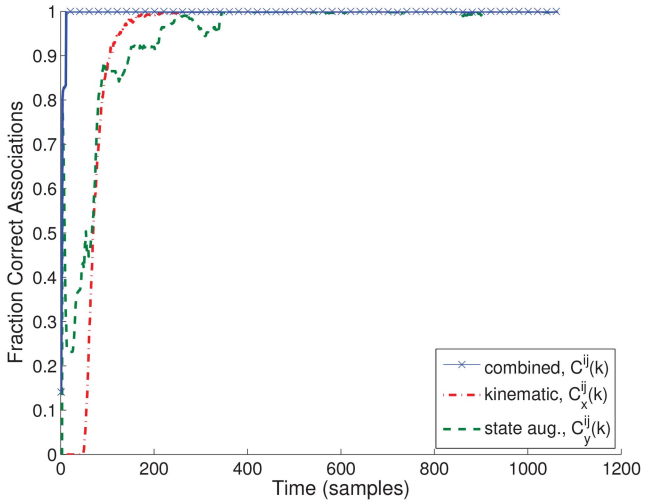

Fig. 19. Average association accuracy over 200 runs (scenario 2A), with window length $L_w = 200$.

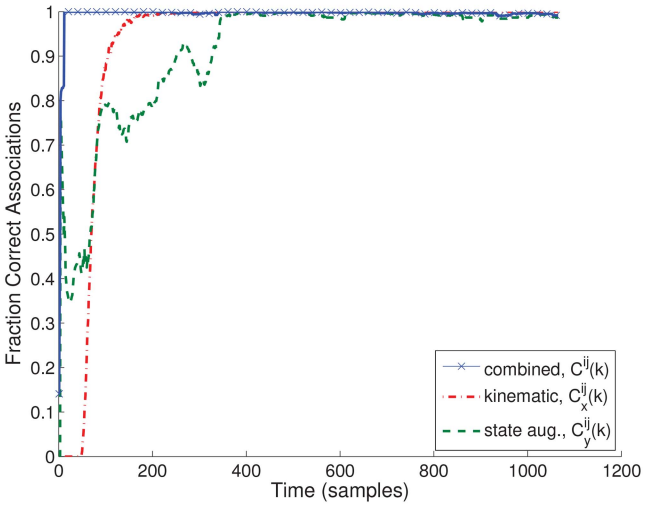

Fig. 20. Average association accuracy over 200 runs (scenario 2B), with window length $L_w = 200$.

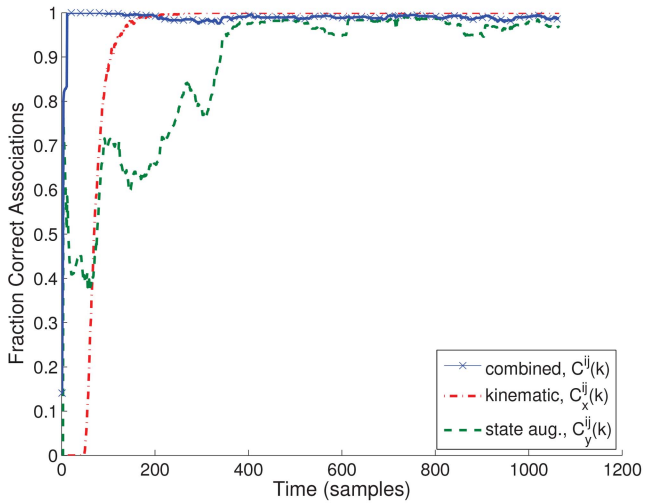

Fig. 21. Average association accuracy over 200 runs (scenario 2C), with window length $L_w = 200$.

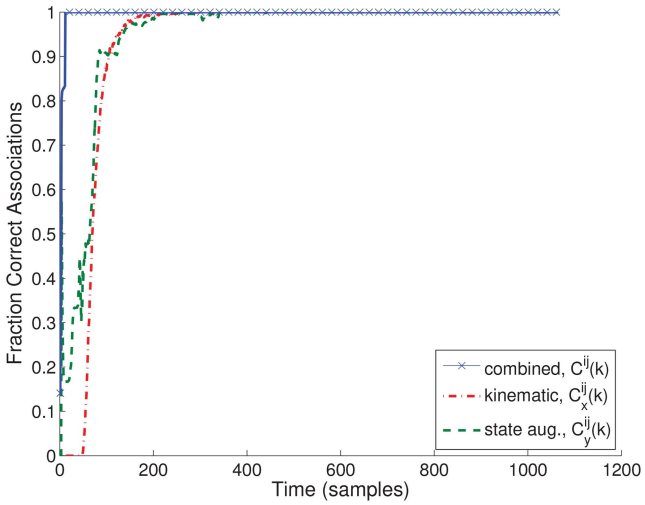

Fig. 22. Average association accuracy over 200 runs with unscented state augmentation costs (scenario 2A), window length $L_w = 200$.

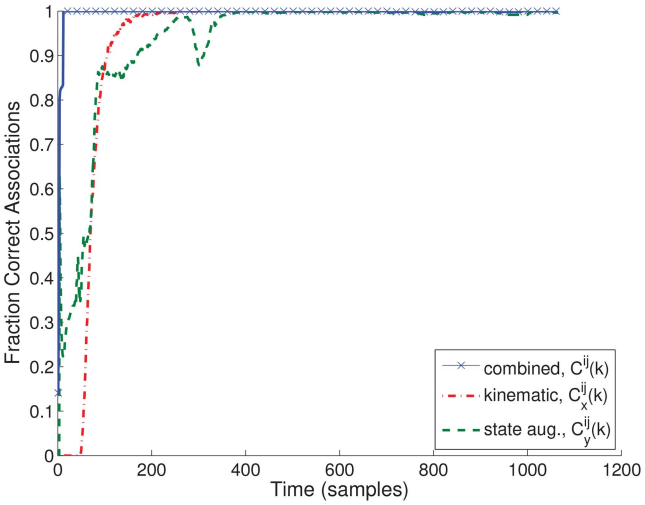

Fig. 23. Average association accuracy over 200 runs with unscented state augmentation costs (scenario 2B), window length $L_w = 200$.

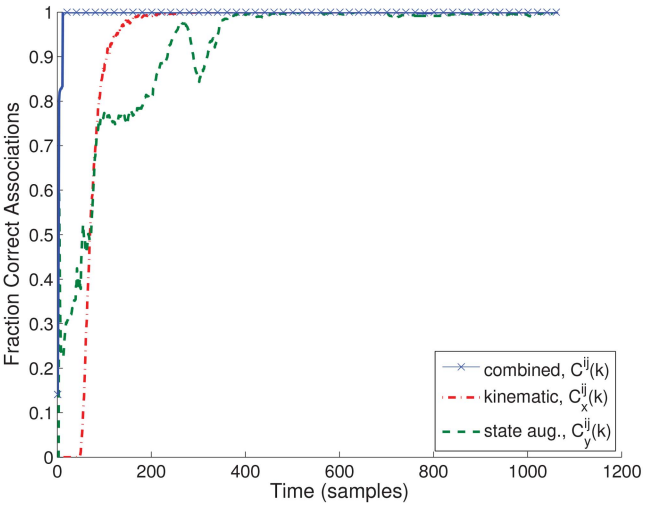

Fig. 24. Average association accuracy over 200 runs with unscented state augmentation costs (scenario 2C), window length $L_w = 200$.

TABLE III
Run Time Comparison of Kinematic Calculations vs. State Augmentation Calculations

	State Augmentation (s)	Kinematic (s)
Direct (1 pt)	2.781	6.003
Unscented (11 pts)	21.597	5.923

A comparison of the computer run time for the kinematic and state augmentation cost calculations for the scenario above is provided in Table III. The simulations were preformed using Matlab 2010b on an Intel Core2 Duo 2.66 GHz processor. The state augmentation cost calculations take longer in the case of the unscented transform since portions of the calculations must be performed at the 11 points used in the transform. The computational complexity of the state augmentation cost will, in general, depend largely on the nature of the state augmentation vector (size, nonlinearities, etc.).

Overall, the best T2TA accuracy is achieved by using the combined cost of association with the unscented transform modification of Section 3.3 to account for the uncertainty in the estimated state augmentation.

7. CONCLUSIONS

Performing T2TA between sensors is necessary to utilize any previously determined information about the tracks of targets from sensors which tracked earlier portions of the target trajectories. Earlier and more accurate association of tracks is desired, as there may be limited time to perform tracking once handover is performed. By utilizing an augmented state of the tracks at the first sensor, T2TA can be performed at the second sensor by combining both kinematic and state augmentation data. Additionally, the need for estimating the same state augmentation of each target directly at the second sensor is circumvented by matching the measured reflectivity of each target at the second sensor with the state augmentation estimated by the first sensor. The main contribution is this use of two nonlinearly related state augmentations and a method of accounting for their uncertainties. The combined cost explicitly allows for complete assignment with different numbers of tracks at each sensor. The combined cost was also found to provide highly accurate association of tracks earlier in a simulated tracking scenario, provided the estimate of the state augmentation is not too inaccurate. The use of very inaccurate state augmentation variables clouds the picture by flattening the likelihoods, deteriorating the association accuracy.

REFERENCES

[1] Y. Bar-Shalom, S. S. Blackman, and R. J. Fitzgerald
Dimensionless score function for multiple hypothesis tracking.
IEEE Transactions on Aerospace and Electronic Systems, **43**, 1 (Jan. 2007), 392–400.

[2] Y. Bar-Shalom and H. Chen
Multisensor track-to-track association for tracks with dependent errors.
Journal of Advances in Information Fusion, **1**, 1 (July 2006), 3–14.

[3] Y. Bar-Shalom, X.-R. Li, and T. Kirubarajan
Estimation with Applications to Tracking and Navigation: Theory, Algorithms and Software.
J. Wiley and Sons, 2001.

[4] Y. Bar-Shalom, P. K. Willett, and X. Tian
Tracking and Data Fusion.
YBS Publishing, 2011.

[5] R. R. Bate, D. D. Muellar, and J. E. White
Fundamentals of Astrodynamics.
New York: Dover Publications, Inc., 1971.

[6] S. Deb, K. Pattipati, and Y. Bar-Shalom
A multisensor-multitarget data association algorithm for heterogeneous sensors.
IEEE Transactions on Aerospace and Electronic Systems, **29**, 2 (Apr. 1997), 560–568.

[7] S. Deb, M. Yeddanapudi, K. Pattipati, and Y. Bar-Shalom
A generalized S-D assignment algorithm for multisensor-multitarget state estimation.
IEEE Transactions on Aerospace and Electronic Systems, **33**, 2 (Apr. 1997), 523–538.

[8] J. Ferry
XMAP: Track-to-track association with metric, feature, and target-type data.
In *Proceedings of the 9th International Conference on Information Fusion*, July 2006, pp. 1–8.

[9] S. J. Julier and J. K. Uhlmann
A new extension of the Kalman filter to nonlinear systems.
In *Proceedings of SPIE International Symposium on Aerospace/Defense Sensing, Simulation and Controls*, Orlando, FL, 1997.

[10] X. R. Li and V. P. Jilkov
A survey of maneuvering target tracking—Part II: Ballistic target models.
In *Proceedings of SPIE Conference on Signal and Data Processing of Small Targets*, San Diego, CA, Aug. 2001.

[11] M. Longbin, S. Xiaoquan, Z. Yiyu, S. Z. Kang, and Y. Bar-Shalom
Unbiased converted measurements for tracking.
IEEE Transactions on Aerospace and Electronic Systems, **34**, 3 (July 1998), 1023–1027.

[12] K. R. Pattipati, R. L. Popp, and T. Kirubarajan
Survey of assignment techniques for multitarget tracking.
In *Multitarget-Multisensor Tracking: Advances and Applications* vol. III, Y. Bar-Shalom and W. D. Blair, Eds., Dedham, MA: Artech House, 2000, ch. 2.

[13] R. L. Popp, K. R. Pattipati, and Y. Bar-Shalom
Dynamically adaptable *m*-best 2-D assignment algorithm and multilevel parallelization.
IEEE Transactions on Aerospace and Electronic Systems, **35**, 4 (Oct. 1999), 1145–1160.

Richard W. Osborne, III obtained his B.S. and M.S. degrees in electrical engineering from the University of Connecticut in 2004 and 2007, respectively.

He is a graduate student currently working on his Ph.D. in electrical engineering at the University of Connecticut, Storrs, CT. His academic interests include target tracking, data fusion, and other areas of estimation.

Yaakov Bar-Shalom (S'63—M'66—SM'80—F'84) was born on May 11, 1941. He received the B.S. and M.S. degrees from the Technion, Israel Institute of Technology, in 1963 and 1967 and the Ph.D. degree from Princeton University, Princeton, NJ, in 1970, all in electrical engineering.

From 1970 to 1976 he was with Systems Control, Inc., Palo Alto, CA. Currently he is Board of Trustees Distinguished Professor in the Department of Electrical and Computer Engineering and Marianne E. Klewin Professor in Engineering. He is also director of the ESP Lab (Estimation and Signal Processing) at the University of Connecticut. His research interests are in estimation theory and stochastic adaptive control and he has published over 360 papers and book chapters in these areas. In view of the causality principle between the given name of a person (in this case, "(he) will track," in the modern version of the original language of the Bible) and the profession of this person, his interests have focused on tracking.

He coauthored the monograph *Tracking and Data Association* (Academic Press, 1988), the graduate text *Estimation with Applications to Tracking and Navigation* (Wiley, 2001), the text *Multitarget-Multisensor Tracking: Principles and Techniques* (YBS Publishing, 1995), and edited the books *Multitarget-Multisensor Tracking: Applications and Advances* (Artech House, Vol. I 1990; Vol. II 1992, Vol. III 2000). He has been elected Fellow of IEEE for "contributions to the theory of stochastic systems and of multitarget tracking." He has been consulting to numerous companies, and originated the series of Multitarget Tracking and Multisensor Data Fusion short courses offered at Government Laboratories, private companies, and overseas.

During 1976 and 1977 he served as associate editor of the *IEEE Transactions on Automatic Control* and from 1978 to 1981 as associate editor of *Automatica*. He was program chairman of the 1982 American Control Conference, general chairman of the 1985 ACC, and cochairman of the 1989 IEEE International Conference on Control and Applications. During 1983–1987 he served as chairman of the Conference Activities Board of the IEEE Control Systems Society and during 1987–1989 was a member of the Board of Governors of the IEEE CSS. Currently he is a member of the Board of Directors of the International Society of Information Fusion and served as its Y2K and Y2K2 President. In 1987 he received the IEEE CSS distinguished Member Award. Since 1995 he is a distinguished lecturer of the IEEE AESS. He is corecipient of the M. Barry Carlton Awards for the best paper in the *IEEE Transactions on Aerospace and Electronic Systems* in 1995 and 2000, and received the 1998 University of Connecticut AAUP Excellence Award for Research, the 2002 J. Mignona Data Fusion Award from the DoD JDL Data Fusion Group, the 2008 IEEE D. J. Picard Medal for Radar Technologies and Applications, and the 2012 Connecticut Medal of Technology.

Peter Willett (F'03) received his B.A.Sc. (engineering science) from the University of Toronto in 1982, and his Ph.D. degree from Princeton University in 1986.

He has been a faculty member at the University of Connecticut since 1986, and since 1998 has been a professor. He has published 135 journal articles (13 more under review), 290 conference papers, and 9 book chapters. His primary areas of research have been statistical signal processing, detection, machine learning, data fusion and tracking. He has interests in and has published in the areas of change/abnormality detection, optical pattern recognition, communications and industrial/security condition monitoring.

He is editor-in-chief for *IEEE Transactions on Aerospace and Electronic Systems*, and until recently was associate editor for three active journals—*IEEE Transactions on Aerospace and Electronic Systems* (for Data Fusion and Target Tracking) and *IEEE Transactions on Systems, Man, and Cybernetics*, parts A and B. He is also associate editor for the IEEE AES Magazine, editor of the AES Magazine's periodic Tutorial issues, associate editor for ISIF's electronic *Journal of Advances in Information Fusion*, and is a member of the editorial board of IEEE's Signal Processing Magazine. He was a member of the IEEE AESS Board of Governors 2003–2009. He was general cochair (with Stefano Coraluppi) for the 2006 ISIF/IEEE Fusion Conference in Florence, Italy, Program Co-Chair (with Eugene Santos) for the 2003 IEEE Conference on Systems, Man & Cybernetics in Washington, D.C., and program cochair (with Pramod Varshney) for the 1999 Fusion Conference in Sunnyvale. He was coorganizer of the tracking subsession at the 1999 IEEE Aerospace Conference, and has been organizer of the Remote Sensing Track of that conference 2000–2003. Jointly with T. Kirubarajan he has coorganized the SPIE "System Diagnosis and Prognosis: Security and Condition Monitoring Issues" Conference in Orlando, 2001–2003. He has been a member of the IEEE Signal Processing Society's Sensor-Array & Multichannel (SAM) Technical Committee since 1997, and both serves on that TC's SAM Conferences' Program Committees and maintains the SAM website.